ACS APPLIED MATERIALS & INTERFACES

RESEARCH ARTICLE

www.acsami.org

Effect of Cellulose Acetate Butyrate Microencapsulated Ammonium Polyphosphate on the Flame Retardancy, Mechanical, Electrical, and Thermal Properties of Intumescent Flame-Retardant Ethylene−Vinyl Acetate Copolymer/Microencapsulated Ammonium Polyphosphate/Polyamide-6 Blends

Bibo Wang,[†] Qinbo Tang,[†] Ningning Hong,[†] Lei Song,[†] Lei Wang,[†] Yongqian Shi,[†] and Yuan Hu*[,†,‡]

[†]State Key Laboratory of Fire Science, University of Science and Technology of China, 96 Jinzhai Road, Hefei, Anhui 230026, People's Republic of China

[‡]Suzhou Key Laboratory of Urban Public Safety, Suzhou Institute for Advanced Study, University of Science and Technology of China, 166 Ren'ai Road, Suzhou, Jiangsu 215123, People's Republic of China

ABSTRACT:

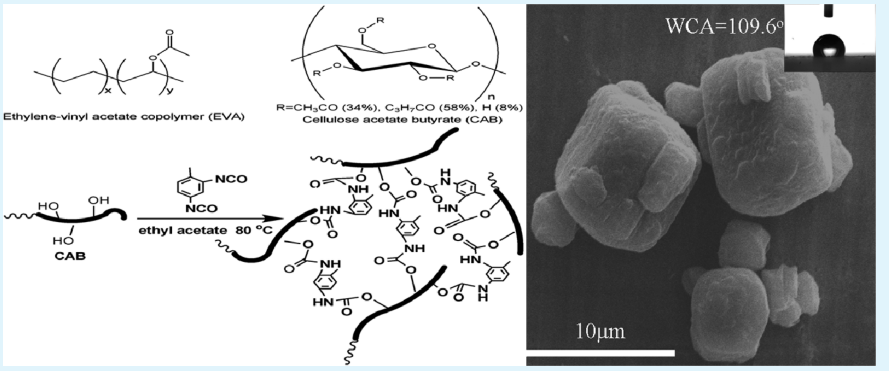

Ammonium polyphosphate (APP), a widely used intumescent flame retardant, has been microencapsulated by cellulose acetate butyrate with the aim of enhancing the water resistance of APP and the compatibility between the ethylene−vinyl acetate copolymer (EVA) matrix and APP. The structure of microencapsulated ammonium polyphosphate (MCAPP) was characterized by Fourier transform infrared spectroscopy (FTIR), X-ray photoelectron spectroscopy (XPS), scanning electron microscopy (SEM), and water contact angle (WCA). The flame retadancy and thermal stability were investigated by a limiting oxygen index (LOI) test, UL-94 test, cone calorimeter, and thermogravimetric analysis (TGA). The WCA results indicated that MCAPP has excellent water resistance and hydrophobicity. The results demonstrated that MCAPP enhanced interfacial adhesion, mechanical, electrical, and thermal stability of the EVA/MCAPP/polyamide-6 (PA-6) system. The microencapsulation not only imparted EVA/MCAPP/PA-6 with a higher LOI value and UL-94 rating but also could significantly improve the fire safety. Furthermore, the microencapsulated EVA/MCAPP/PA-6 composites can still pass the UL-94 V-0 rating after treatment with water for 3 days at 70 °C, indicating excellent water resistance. This investigation provides a promising formulation for the intumescent flame retardant EVA with excellent properties.

KEYWORDS: microencapsulation, ethylene−vinyl acetate copolymer, cellulose acetate butyrate, flame retardancy, mechanical properties, electrical property, thermal properties

1. INTRODUCTION

Ethylene−vinyl acetate copolymer (EVA) is widely used in many fields, especially in the cable industry as excellent insulating materials, owing to its good physical and mechanical properties.[1] However, the inherent flammability of EVA, with a typical limiting oxygen index (LOI) of 17, limits its application in some fields like electronic appliances where high flame retardancy is required. Among the many ways of flame retardation of EVA, intumescent flame retardants (IFRs) have been considered to be a promising method, which is because they are low toxicity, low smoke, halogen free, and also very efficient.[2−4]

In spite of many advantages, IFRs may reduce the mechanical properties and other properties of the materials because the rather different polarities of IFRs and EVA make them thermodynamically immiscible. Meanwhile, the differences in polarity cause a weak interfacial adhesion, which plays an important role in the mechanical and other related properties. Furthermore, this IFR system is moisture sensitive and thus is easily attacked by

Received: July 19, 2011
Accepted: August 22, 2011
Published: August 22, 2011

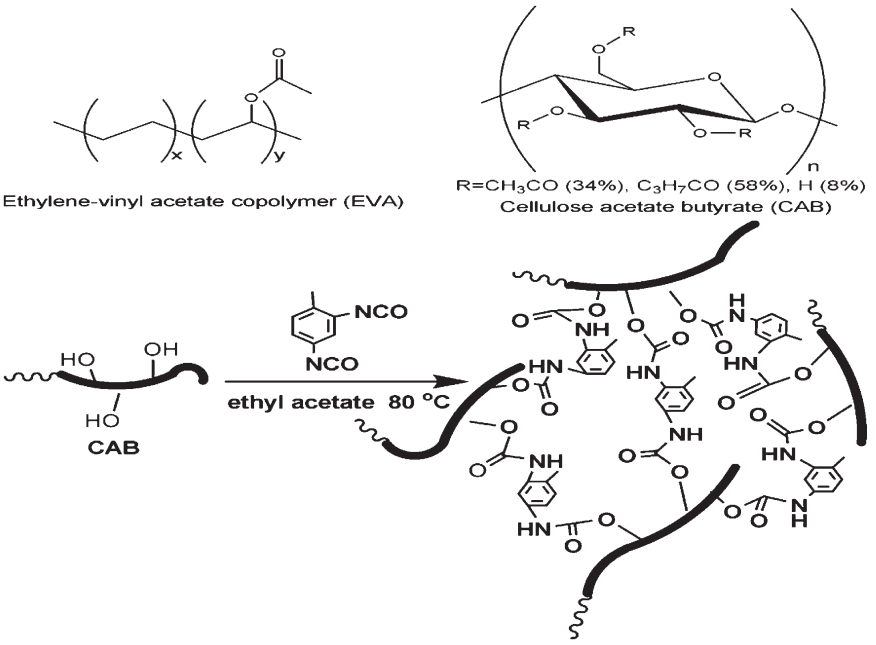

Figure 1. Reaction scheme of the shell of MCAPP microcapsules.

water and exuded during the service life, resulting in a decrease in the flame-retardant properties of the polymer composites. To deal with the above problems, several methods can be employed, such as modifying the surface by the silane coupling agent[5,6] and different compatibilizer[7−11] for improving the dispersion. These methods have been proven to be effective methods for improving the interfacial adhesion and morphology control in a variety of incompatible blends. However, the problems of water resistance and exudation of IFRs during the service life have not been effectively solved.

In order to overcome these problems, the technique of microencapsulation is a good choice. The encapsuling substances can be selected from abundant natural to synthetic materials, which depend on the properties desired in the final microcapsules. In our previous work, microencapsulated ammonium polyphosphate (APP) with water-insoluble polymers such as, melamine−formaldehyde (MF) or polyurethane (PU), by the in situ polymerization method were investigated and reported.[12,13] The results suggested that the microencapsulated ammonium polyphosphate can significantly increase the water resistance of APP and the interfacial adhesion between APP particles and the polymer matrix. Li et al. reported expandable graphite (EG) microencapsulated by polymethyl methacrylate (PMMA) through in situ emulsion polymerization; the pEG-PMMA particles with −COOH groups can react with the R-NCO groups of isocyanurate to synthesize pEG-PMMA/RPUF with favorable compatibility and mechanical properties.[14]

Cellulose esters are prepared from the esterification of renewable and biodegradable cellulose which is abundant in agricultural wastes such as straws and residues or so-called biomasses. Recently, cellulose esters have been widely reported as a microcapsule material.[15−20] That is because cellulose esters have many excellent properties, such as very low toxicity, high stability, high T_g, film strength, compatibility with a wide range of actives, and ability to form micro- and nanoparticles. Cellulose acetate butyrate (CAB) esterified by acetyl and butyryl groups (Figure 1) is a brittle and transparent material. Not all of the original cellulose OH groups are converted in the esterification process, and esterification may occur at any of the three original OH position. Therefore, the thermo-chemical and physical properties of the CAB polymeric film can be improved by cross-linking CAB with a diisocyanate via the urethane bond formation.[21] Moreover, both the CAB and EVA have the same acetyl group, which may have similar polarity. According to the theory of similarity and intermiscibility, if we use CAB microencapsulated IFRs, the CAB shell material may increase the water resistance of IFRs and enhance the compatibility and dispersion betweem EVA matrix and CAB microencapsulated IFRs.

The goal of this work is to provide a formulation for the EVA with excellent properties through microencapsulation technology. In this study, first, CAB microencapsulated ammonium polyphosphate (MCAPP) was prepared. Polyamide-6 (PA-6) was chosen as carbon source, which has been proven to be an effective carbonization agent.[22,23] Then, MCAPP and PA-6 were used as intumescent flame retardants for EVA and were considered to be the CAB microencapsulation technology on the mechanical, electrical, thermal, and flame retardant properties of intumescent flame-retardant systems.

2. EXPERIMENTAL SECTION

2.1. Materials. Cellulose acetate butyrate (CAB) was purchased from Wenhua Chemical Company (Shanghai, China); the acetyl, butyryl, and hydroxyl contents are 34%, 58%, and 8%, respectively. Ethylene−vinyl acetate copolymer (containing 28 wt % vinyl acetate), ammonium polyphosphate (APP), and polyamide-6 (PA-6) were supplied by Samsung Total Petrochemical (Korea), Shandong Shian Chemical Co., Ltd. (Shangdong, China), and Ube Company (Japan), respectively. Alkylphenol polyoxyethylene (OP-10) surfactant was provided by Haijie Zibo Chemical Co., Ltd. Ethyl acetate (CP) and toluene-2,4-diisocyanate (TDI, AP) were supplied by Sinopharm Chemical Reagent Co., Ltd. (Shanghai, China).

2.2. Preparation of Cellulose Acetate Butyrate Microencapsulated Ammonium Polyphosphate (MCAPP). Four grams

Table 1. Formulation of Flame Retardant EVA Composites

sample	EVA (wt%)	APP (wt%)	MCAPP (wt%)	PA-6 (wt%)	LOI	UL-94
EVA0	100				17	no rating
EVA1	70		24	6	30.5	V-2
EVA2	70		22.5	7.5	31	V-0
EVA3	70		20	10	28.5	V-2
EVA4	70	22.5		7.5	30	V-2
EVA5	70	24		6	29	V-2

of CAB and 150 mL of ethyl acetate were put into a three-neck bottle with a stirrer. The mixture was heated to about 80 °C and kept at that temperature. After CAB was dissloved in ethyl acetate, 60 g of APP and 0.6 g of OP-10 were added and stirred for 15 min. Then, 4 g of TDI was added dropwise to the mixture. The resulting mixture was kept at 80 °C for 6 h. After that, the mixture was cooled to room temperature, filtered, washed with ethyl acetate, and dried at 80 °C, and the MCAPP powder was finally obtained. The theoretical principal polymer repeat unit for shell of MCAPP microcapsules is shown in Figure 1.

2.3. Preparation of Flame Retarded EVA Composites. EVA and PA-6 were blended by a twin-screw extruder LSSHJ-20 (Shanghai Kechuang Plastic Machinery Co., Ltd., China). The screw speed is 160 r/min, and the feed rate is 100 r/min. The processing temperatures are 100, 180, 220, 225, 220, 210, and 200 °C, respectively. After that, EVA, PA-6, and MCAPP blends were prepared in a Brabender-like apparatus at a temperature of 140 °C for 10 min. The model of the "Brabender-like" is LH-60 (Shanghai Kechuang Plastic Machinery Co., Ltd., China). The EVA composites were mixed at 60 r/min with a roller blade. After mixing, the samples were hot pressed at 140 °C under 10 MPa for 5 min into sheets of suitable thickness for analysis. The formulations are given in Table 1.

2.4. Measurements. *X-ray Photoelectron Spectroscopy (XPS).* The X-ray photoelectron spectroscopy measurement was carried out using an ESCALAB MK II (VG Co., Ltd., England) spectrometer, with Al Kα excitation radiation (hν = 1253.6 eV) in ultrahigh vacuum conditions.

Scanning Electron Microscopy (SEM). The morphology of the sample after being gold-sputtered was studied by a PHILIPS XL30E scanning electron microscope. The specimens of EVA composites were cryogenically fractured in liquid nitrogen first and then sputter-coated with a conductive layer. The accelerated voltage was 20 KV.

Water Contact Angle Measurements (WCA). The water CA of the samples was measured with a drop-shape analysis system (Krüss DSA100) at three different points for each.

Solubility in Water. A few samples (about 10 g) were put into 100 mL of distilled water at different temperatures and stirred at that temperature for 2 h. The suspension was then filtered. Fifty milliliters of the filtrate was taken out and dried to constant weight at 105 °C. Solubility of samples in water can be calculated.

Limiting Oxygen Index (LOI). LOI was measured using a HC-2 oxygen index meter (Jiang Ning Analysis Instrument Company, China) on sheets 100 × 6.7 × 3 mm^3 according to the standard oxygen index test ASTM D2863-2010.

UL-94 Vertical Burning Test. The vertical burning test was conducted by a CZF-II horizontal and vertical burning tester (Jiang Ning Analysis Instrument Company, China). The specimens used were 127 × 12.7 × 3 mm^3 according to UL-94 test ASTM D3801-2010.

Determination of Water Resistance of EVA Composite. The specimens used for the flammability test were put in 500 mL of distilled water at 70 °C and were kept at this temperature for various time periods. The specimens were subsequently removed, dried in the vacuum oven, and evaluated by burning tests (UL-94 and LOI).

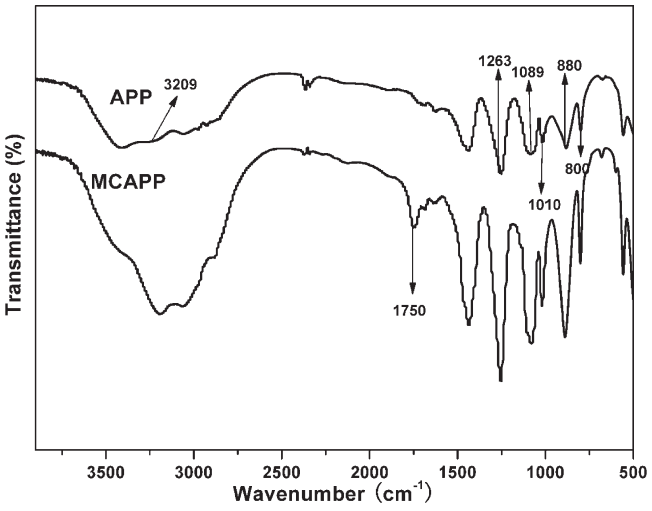

Figure 2. FTIR spectra of APP and MCAPP.

Thermogravimetric Analysis (TGA). Thermogravimetric analysis (TGA) was carried out using a Q5000 IR thermogravimetric analyzer (TA InstrumentsWaters, China) at a linear heating rate of 20 °C min^{-1} in N_2 atmosphere. The weight of all the samples were kept within 5−10 mg. Samples in an open Pt pan were examined under an airflow rate of 6 × 10^{-5} m^3 per minute at a temperature ranging from room temperature to 700 °C.

Mechanical Properties. The mechanical properties were measured with a universal testing machine (Instron 1185) at a temperature of 25 ± 2 °C. The crosshead speed was 20 mm/min. Dumbbell-shaped specimens were prepared according to ASTM D412. The tensile strength and elongation at break were recorded.

Electric Properties. Volume resistivity of the composites was measured at room temperature by a high-insulation resistance meter (Shanghai Precision & Scientific Instrument Co., China). Square samples with an area of 100 × 100 mm^2 were used after they were cut from the molded sheets.

Dynamical Mechanical Thermal Analysis (DMTA). Dynamic mechanical properties were measured with DMA Q800 (TA, USA). The dynamic storage modulus was determined at a frequency of 10 Hz and a heating rate of 5 °C/min over the range of −70 to 75 °C. The dimensions of the samples were approximately 1 mm in thickness, 20 mm in length, and 5 mm in width.

Cone Calorimeter. The combustion test was performed on the cone calorimeter (FTT, UK) test according to ISO 5660 standard procedures, with 100 × 100 × 3 specimens. Each specimen was wrapped in an aluminum foil and exposed horizontally to 35 kW/m^2 external heat flux.

3. RESULTS AND DISCUSSION

3.1. Characterization of MCAPP. The Fourier transform infrared spectroscopy (FTIR) spectra of APP and MCAPP are shown in Figure 2. The typical absorption peaks of APP include 3200 (N−H), 1256 (P−O), 1075 (P−O symmetric stretching vibration), 1020 (symmetric vibration of PO_2 and PO_3), 880 (P−O asymmetric stretching vibration), and 800 (P−O−P) cm^{-1}. The spectrum of MCAPP shows an absorption band at 1750 cm^{-1} for the C═O stretching of cross-linked CAB. Moreover, it is obvious that the NCO absorption band at 2270 cm^{-1} disappears. As a result, cross-linked CAB exists in the structure of MCAPP.

The XPS spectra of APP and MCAPP are shown in Figure 3. It can be seen that the peaks located at 134.7 and 190.9 eV are attributed to P_{2P} and P_{2S} of APP. For MCAPP, the intensities of

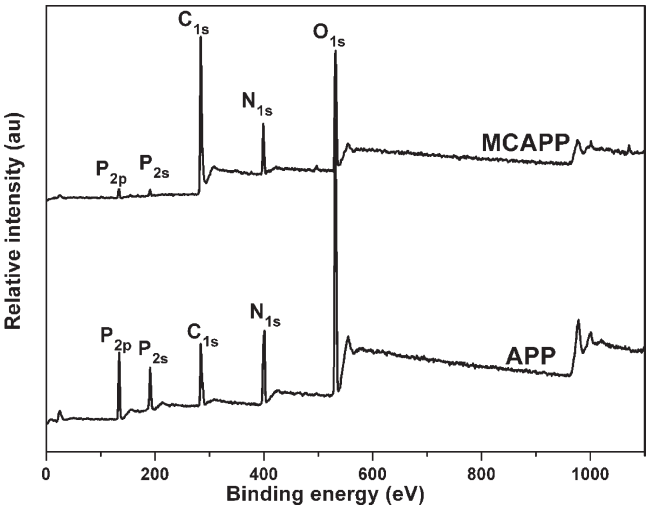

Figure 3. XPS spectra of APP and MCAPP.

Table 2. Surface Elemental Compositions of APP and MCAPP

sample	C (wt%)	O (wt%)	N (wt%)	P (wt%)
APP	22.38	47.29	19.27	11.06
MCAPP	61.71	25.16	11.27	1.86

peaks aforementioned decrease sharply, meanwhile the intensities of the C_{1S} peak centered at 284.7 eV increase greatly. Table 2 shows the surface elemental compositions of MCAPP and APP particles. The P, N, and O atom content of MCAPP are 1.86, 11.27, and 25.16 wt %, which are much lower than those of APP (11.06, 19.27, and 47.29 wt %), and C atom content of MCAPP is 61.71 wt %, higher than that of APP (22.38 wt %). The changes of the above peaks and elemental compositions are due to the coverage of the outside APP particles with the TDI cross-linked cellulose acetate butyrate, which indicates that APP is well coated by the resin.

The surface morphologies of the APP and MCAPP particles are shown in Figure 4. It is clear that the surface of APP particle is very smooth. After microencapsulation, MCAPP presents a comparably rough surface. The surface properties of MCAPP have been evaluated by contact angle measurements using water, on coatings prepared by spin coating of particle suspensions. The water contact angle (WCA) of the native APP is 11.5°, as it absorbed water immediately. However, the reaction between TDI and hydroxyl group of the CAB results in the transformation of hydrophilic to hydrophobic MCAPP surface, with a WCA about 109.6°. The above results also suggest a coating of APP with the cross-linked cellulose acetate butyrate

Figure 5 shows the influence of cellulose acetate butyrate on the solubility of MCAPP. It can be seen that the solubility of APP at 25 and 75 °C is 0.63 and 3.1 g/100 mL H_2O (2 h), respectively, indicating that APP can be easily attacked by moisture or water, especially at high temperatures. After microencapsulation of APP with the cellulose acetate butyrate, the solubility of MCAPP decreases sharply at 25 and 75 °C. The water solubility of MCAPP decreases 80% compared with APP at 25 °C. All these prove that a layer of cellulose acetate butyrate on MCAPP particles can effectively protect the APP from water.

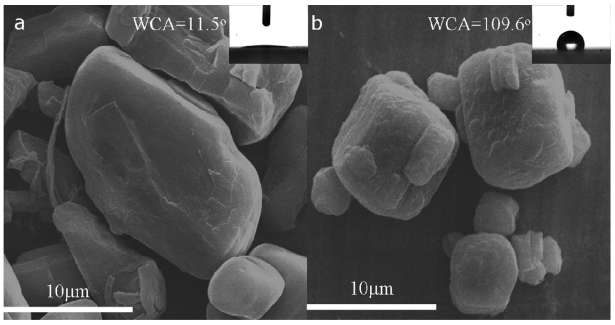

Figure 4. SEM photographs of APP (a) and MCAPP (b) particles. The inset is a picture of water contact angle.

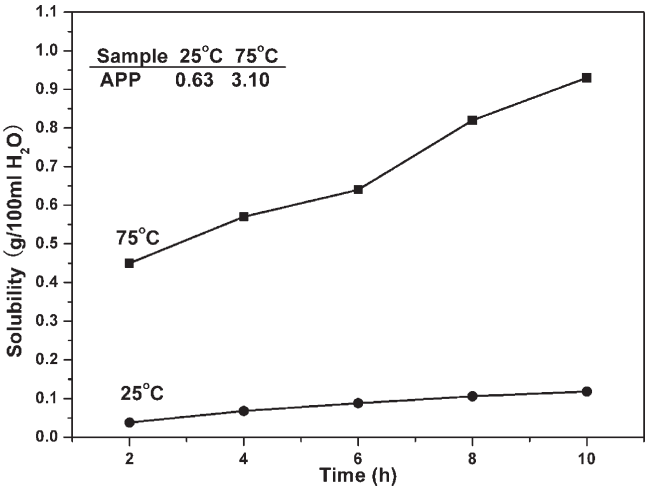

Figure 5. Water solubility of MCAPP after different times.

3.2. Flame Retardancy. LOI, UL-94, and cone calorimeter tests are widely used to determine the flammability of flame retardant materials. LOI, the minimum oxygen concentration by volume for maintaining the burning of a material, is a important parameter for evaluating the flame retardancy of a polymeric material. Usually, there is a complex correlation among LOI value, UL-94 rating, and cone result.[24] The LOI values and UL-94 testing results of the EVA composites are presented in Table 1. The experimental results of vertical burning rate show that the EVA/MCAPP/PA-6 systems give a V-2 rating when the weight ratio of MCAPP to PA-6 is 4:1 and 2:1 with 30 wt % loadings. When the weight ratio of MCAPP to PA-6 is 3:1, the EVA composites can reach UL-94 V-0 rating and the LOI value can be as high as 31. However, with the same loading and formulation, the EVA/APP/PA-6 system can only pass V-2 rating and the LOI value is 30. It can be clearly found that EVA/MCAPP/PA-6 systems have higher flame retardancy and vertical burning rate than those of EVA/APP/PA-6.

The cone calorimeter based on the oxygen consumption principle has been widely used to evaluate the combustion behaviors of materials and products since it is developed at the NBS (now NIST) in 1982. Although the cone calorimeter is a small-scale test, some of its results have been found to correlate well with those obtained from large scale fire tests and can be used to predict the behavior of materials in real fires. Heat release rate (HRR) results of EVA and flame retardant EVA composites are shown in Figure 6, and the related total heat release (THR),

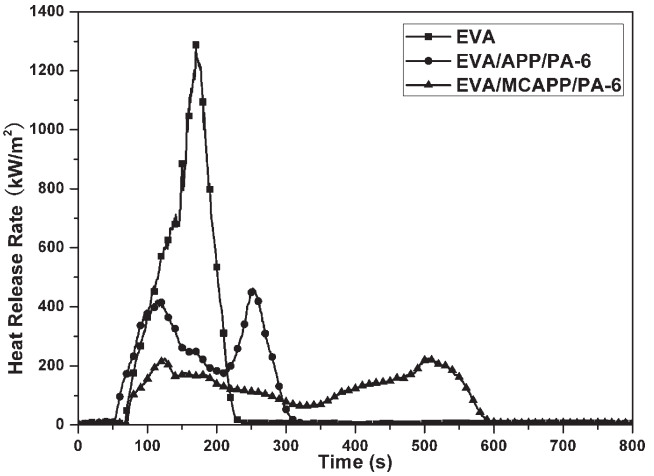

Figure 6. Heat release rate curves of EVA and flame retardant EVA composites.

Table 3. Related Cone Date of EVA and Flame Retardant EVA Composites

sample	TTI (s)	time to PHRR (s)	PHRR (KW/m^2)	THR (MJ/m^2)	FPI (m^{2}s/KW)	FGI (KW/sm^2)
EVA	55	170	1287.45	97.48	0.04	7.57
EVA/APP/PA-6	37	252	461.14	67.03	0.08	1.83
EVA/MCAPP/PA-6	55	502	225.73	71.30	0.24	0.45

peak HRR (PHRR), time to ignition (TTI), and time to peak HRR are recoded in Table 3. It can be found that pure EVA burns out within 230 s after ignition. A very sharp HRR peak appears at the range of 50−230 s with a peak heat release rate (pk-HRR) of 1287.45 kW/m^2. However, the flame retardant EVA composites show dramatic decline of the HRR peaks and prolongation of the combustion time. The pk-HRR value for EVA/MCAPP/PA-6 is 225.73 kW/m^2, much lower than 461.14 kW/m^2 for EVA/APP/PA-6. The HRR curve of flame retardant EVA composites exhibit two peaks. The first peak is assigned to the ignition and to the formation of an expanded protective shield; the second peak is explained by the destruction of the intumescent structure and the formation of a carbonaceous residue, whereas the HRR curve of EVA/MCAPP/PA-6 composite is very flat after the first peak. Also, the combustion time of EVA/MCAPP/PA-6 prolongs to 590 s that is much larger than 310 s of the EVA/APP/PA-6 composite. From the above discussion, it can be concluded that the microencapsulation can significantly decrease the HRR and prolong the combustion time. The EVA/MCAPP/PA-6 composite has a little higher THR than that of EVA/MCAPP/PA-6 composite. The reason may be due to the fact that the actual amount of flame retardant after microencapsulation is lower than that of the one without microencapsulation. In order to judge the fire hazard more clearly, the fire performance index (FPI) and the fire growth index (FGI) were selected. The former is defined as the proportion of TTI and the peak HRR. It is reported that there is a certain correlation between the value of FPI of material and the time to flashover. When the value of FPI reduces, the time to flashover will be advanced. Thus, it is generally accepted that the value of FPI of a material is smaller and its fire risk is higher. The latter is defined as the proportion of peak HRR and the time to peak HRR. According to the previous report, the larger the value of FGI, the shorter time it takes to arrive at a high peak HRR and the more fire hazard the materials have. The comparison between the values of FPI and FGI of the EVA specimens has been shown in Table 3. Apparently, the fire risk of EVA/MCAPP/PA-6 composite is much smaller than that of EVA/APP/PA-6 composite.

Table 4. UL-94 Testing Results and LOI Values of EVA Composites after Water Treatment at 70 °C for Several Hours

	EVA/APP/PA-6 (EVA4)		EVA/MCAPP/PA-6 (EVA2)	
time (h)	UL-94	LOI	UL-94	LOI
0	V-2	30	V-0	31
24	NR	27	V-0	29.5
72	NR	24	V-0	27.5

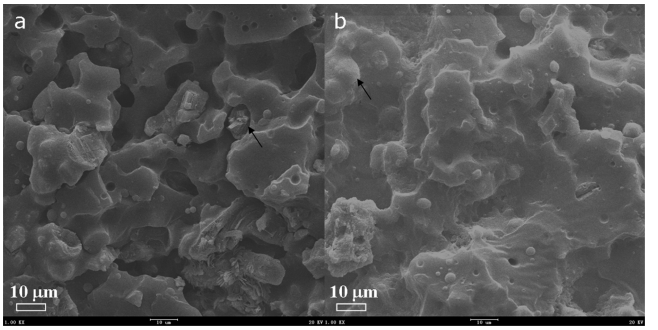

Figure 7. SEM images for EVA/APP/PA-6 and EVA/MCAPP/PA-6.

In order to examine the water resistance of the flame retardant EVA composites, the EVA composites with 22.5 wt % MCAPP and 7.5 wt % PA-6 are treated with water at 70 °C for different times and their flame retardant properties are evaluated (Table 4). The EVA/APP/PA-6 composite burns completely and is considered to be a no rating material after water treatment for 24 h. However, it can be seen that the EVA/MCAPP/PA-6 has a good water-resistant property. Although the LOI value drops from 31 to 27.5 after water treatment for 72 h, the sample can still pass the UL-94 V-0 test. This is because the MCAPP has excellent water resistance according to the result of water solubility of MCAPP.

From the above results, it can be found the MCAPP not only increases the flame retardancy of EVA/MCAPP/PA-6 composite but also enhances its water-resistant property. Therefore, in the following work, the interfical adhesion, mechanical, electrical, and thermal stability of EVA/MCAPP/PA-6 (70/22.5/7.5) blends are studied.

3.3. Morphology. The SEM images of fracture sections for EVA/APP/PA-6 and EVA/MCAPP/PA-6 blends are shown in Figure 7. Obvious differences can be found in Figure 7. Without microencapsulation, the interfaces between flame retardant APP and the polymeric matrix are clearly apparent because the images showed many large APP particles or cavities where APP resided as a result of sample fabrication in the matrix. The samples for SEM measurements were fabricated through the cryopreservation-brittle-breaking method because of the interface adhesion

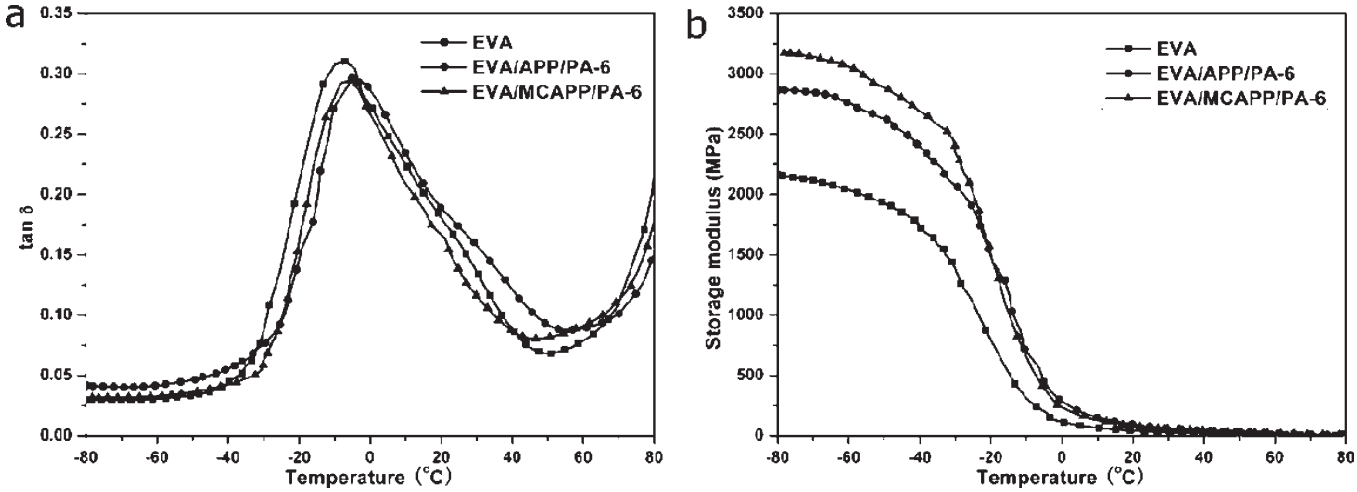

Figure 8. Temperature dependence of tan δ (a) and storage modulus (b) of EVA and flame retardant EVA composites.

force between the matrix and APP; consequently, APP is rather easy to drop, and cavities subsequently formed. After being microencapsulated with CAB, for the EVA/MCAPP/PA-6 system, the MCAPP has well dispersion in the polymeric matrix and almost no obvious interfaces are observed between fillers and the matrix. As expected, the CAB shell can enhance the dispersion of MCAPP and the compatibility betweem EVA matrix and MCAPP, because both CAB shell and EVA have acetyl group and similar polarity. Because the CAB has increased the interfical adhesion between the MCAPP and polymer matrix, it will also result in changed mechanical and electrical properties, which will be analyzed in the following sections.

3.4. Dynamical Mechanical Thermal Analysis. The tan δ and storage modulus of EVA and flame retardant EVA composites are shown in Figure 8. The temperature at maximum of tan δ is usually taken as the glass transition temperature (T_g). In contrast to the pure EVA (−7.1 °C), that of the flame retardant EVA composite shifts toward high temperature (Figure 8a). It can be observed that the T_g value of EVA/APP/PA-6 is −5.1 °C, because the rigid filler APP limits the mobility of the polymer chains. After microencapsulation, the T_g of EVA/MCAPP/PA-6 shifts to −5.5 °C. This may be because APP is microencapsulated by the flexible CAB shell which also has plasticization effects. The storage modulus of EVA and flame retardant EVA composites, as a function of temperature, are shown in Figure 7b. Above 0 °C, there are no obvious differences in modulus for the three materials, while below 0 °C, the flame retardant EVA composites have higher storage modulus than that of EVA. This is because the rigid filler has imparted stiffness behavior to the filled EVA composites. Moreover, the storage modulus of EVA/MCAPP/PA-6 has higher value than that of EVA/APP/PA-6, which indicates that microencapsulation enhances the compatibility between the APP and the matrix system.

3.5. Mechanical Properties. Table 5 shows the tensile strength and elongation at break of EVA and flame retardant EVA composites. Before microencapsulation, both the tensile strength and elongation at break decrease obviously. The tensile strength value and around the elongation at break of EVA are 19.6 MPa and 740%, while being 13.6 MPa and 510%, respectively, for EVA/APP/PA-6. However, after microencapsulation, the tensile strength and elongation at break are evidently increased in comparison with unmicroencapsulated samples, although the mechanical properties are lower than those of pure EVA.

Table 5. Tensile Strength, Elongation at Break, and Volume Resistivity of EVA and Flame Retardant EVA Composites

sample	tensile strength (MPa)	elongation at break (%)	volume resistivity (Ω·cm)
EVA	19.6	740	1.54×10^{15}
EVA/APP/PA-6	13.6	510	1.9×10^{14}
EVA/MCAPP/PA-6	14.8	590	5.4×10^{14}

3.6. Electrical Properties. Resistivity studies are very important for insulating materials, which is because that the most desirable character of an insulator is its ability to resist the leakage of electrical current. The electrical properties of pure EVA and flame retardant EVA composites are listed in Table 5. It can be noted that the volume resistivity of the EVA/APP/PA-6 composite decreases significantly compared to the pure EVA. After microencapsulation, the EVA/APP/PA-6 composite shows higher volume resistivity than that of unmicroencapsulated sample. This is because APP is microencapsulated by CAB shell, which can be considered as an insulating shield to isolate the APP from the EVA matrix. As a result, a whole conductive pathway cannot be generated. Therefore, the microencapsulated APP flame retardant EVA composite has higher volume resistivity than that of unmicroencapsulated sample.

3.7. Thermal Stability. Furthermore, TGA and DTG curves of EVA and flame retardant EVA composites under N_2 atmosphere are shown in Figure 9, and the related TGA data are recorded in Table 6. It can be found that the thermal degradation of pure EVA are composed of two main steps. The maximum weight loss temperatures (T_{max}) for the two decomposition steps are 350.0 and 471.9 °C, respectively. Compared with pure EVA, the initial degradation temperature (the initial degradation temperature is defined as $T_{-5wt\%}$, where 5 wt % mass loss takes place in our laboratory) of flame retardant EVA composites decreases, owing to the thermal degradation of intumescent flame retardant. The flame retardant EVA composites exhibit an enhanced thermal behavior at temperatures ranging from 350 to 700 °C and have higher residues. Compared with the

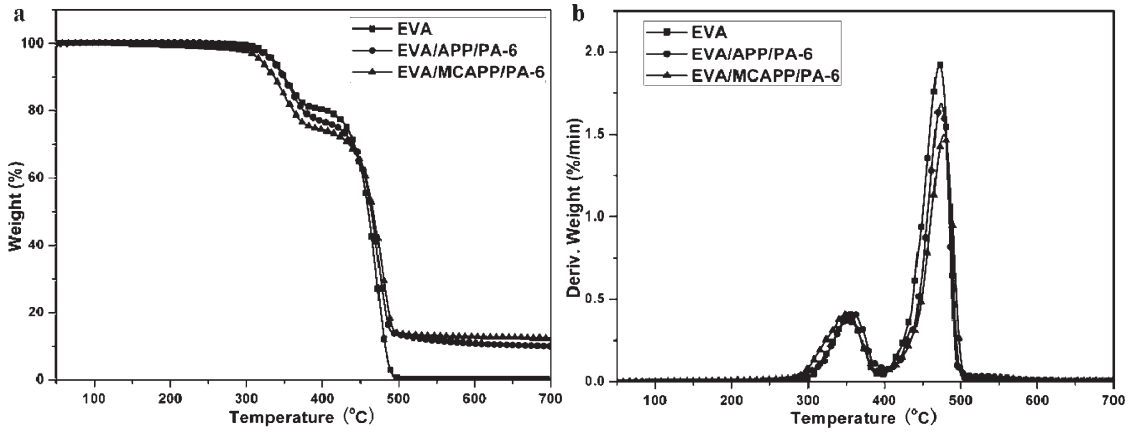

Figure 9. TGA (a) and DTG (b) curves of EVA and flame retardant EVA composites in nitrogen.

Table 6. TGA Data of EVA and Flame Retardant EVA Composites

		T_{max} (°C)		
sample	$T_{-5\%}$ (°C)	first step	second step	residues at 700 °C (%)
EVA	335.6	350.0	471.9	0.4
EVA/APP/PA-6	333.7	358.8	474.0	10.0
EVA/MCAPP/PA-6	318.8	351.4	477.9	12.3

EVA/APP/PA-6, the microencapsulated samples have lower initial degradation temperature and T_{1max}. However, the microencapsulated sample have higher T_{2max} and residues than those of the unmicroencapsulated one. This may be due to the fact that the CAB shell materials can serve as char source, which can react with APP to form more intumescent char. The higher char residue is produced, the higher are the barrier properties of heat and gas transfer between EVA matrix and combustion zone obtained. Therefore, the EVA/MCAPP/PA-6 composite has better thermal stability than that of the EVA/APP/PA-6 composite at the higher temperature range.

4. CONCLUSION

CAB was employed as the shell material for microencapsulated APP, and the MCAPP demonstrated excellent water resistance and hydrophobicity. The results also indicated that EVA/MCAPP/PA-6 has better flame retardancy and thermal stability than those of EVA/APP/PA-6. Moreover, the water resistance of the flame-retardant composites was also studied. The result showed that the EVA/MCAPP/PA-6 can still retain UL-94 V-0 rating after treatment with water for 3 days at 70 °C, which indicated an excellent water resistance. Because both CAB and EVA have an acetyl group, the CAB shell could enhance the dispersion of MCAPP and the compatibility between EVA matrix and MCAPP. Furthermore, the EVA/MCAPP/PA-6 composite demonstrated higher mechanical, dynamical mechanical, and electrical properties than those of EVA/APP/PA-6 composite. That is because the microencapsulated shell material can not only enhance the interfacial adhesion between the fillers and EVA matrix but also act as an insulating shield to isolate the APP from the EVA matrix. In summary, the EVA/MCAPP/PA-6 system developed in this study may be a promising formulation for intumescent flame retardant EVA with excellent properties.

AUTHOR INFORMATION

Corresponding Author

*Fax/Tel: +86-551-3601664. E-mail: yuanhu@ustc.edu.cn.

ACKNOWLEDGMENT

The work was financially supported by the Program for Specialized Research Fund for the Doctoral Program of Higher Education (200803580008), the Youth Innovation Fund of USTC, the Program for Science and Technology of SuZhou (SG-0841), and the joint fund of Guangdong province and CAS (No.2010A090100017).

REFERENCES

(1) Holmes, M. *Plast. Addit. Compd.* **2004**, *6*, 32–36.
(2) Heinrich, H.; Stefan, P. *Polym. Int.* **2000**, *49*, 1106–1114.
(3) Bourbigot, S.; Le, B. M.; Duquesne, S.; Rochery, M. *Macromol. Mater. Eng.* **2004**, *289*, 499–511.
(4) Wang, B. B.; Tai, Q. L.; Nie, S. B.; Zhou, K. Q.; Tang, Q. B.; Hu, Y.; Song, L. *Ind. Eng. Chem. Res.* **2011**, *50*, 596–605.
(5) Castel, C. D.; P., T., Jr; Barbosa, R. V.; Liberman, S. A.; Mauler, R. S. *Composites, Part. A: Appl. Sci. Manuf.* **2010**, *41*, 185–191.
(6) Liauw, C. M.; Lees, G. C.; Hurst, S. J.; Rothon, R. N.; Ali, S. *Composites, Part. A: Appl. Sci. Manuf.* **1998**, *29*, 1313–1318.
(7) Chiang, W. Y.; Hu, C. H. *Composites, Part. A: Appl. Sci. Manuf.* **2001**, *32*, 517–524.
(8) Liu, S. P.; Ying, J. R.; Zhou, X. P.; Xie, X. L.; Mai, Y. W. *Compos. Sci. Technol.* **2009**, *69*, 1873–1879.
(9) Kusmono, Z. A.; Ishak, M.; Chow, W. S.; Takeichi, T. *Composites, Part. A: Appl. Sci. Manuf.* **2008**, *39*, 1802–1814.
(10) Zhang, L.; Li, C. Z.; Zhou, Z. L.; Shao, W. *J. Mater. S.* **2007**, *42*, 4227–4232.
(11) Song, P. G.; Shen, Y.; Du, B. X.; Peng, M.; Shen, L.; Fang, Z. P. *Appl. Mater. Interfaces* **2009**, *1*, 452–459.
(12) Wu, K.; Song, L.; Wang, Z. Z.; Hu, Y. *Polym. Adv. Technol.* **2008**, *19*, 1914–1921.
(13) Ni, J. X.; Song, L.; Hu, Y.; Zhang, P.; Xing, W. Y. *Polym. Adv. Technol.* **2009**, *20*, 999–1005.
(14) Ye, L.; Meng, X. Y.; Ji, X.; Li, Z. M.; Tang, J. H. *Polym. Degrad. Stab.* **2009**, *94*, 971–979.
(15) Babu, V. R.; Kanth, V. R.; Mukund, J. M.; Aminabhavi, T. M. *J. Appl. Polym. Sci.* **2010**, *115*, 3542–3549.
(16) Bahri, Z. E.; Taverdet, J. L. *J. Appl. Polym. Sci.* **2007**, *103*, 2742–2751.

(17) Junyaprasert, V. B.; Manwiwattanakul, G. *Int. J. Pharm.* **2008**, *352*, 81–91.
(18) Fundueanu, G.; Constantin, M.; Esposito, E.; Cortesi, R.; Nastruzzi, C.; Menegatti, E. *Biomaterials* **2005**, *26*, 4337–4347.
(19) Edgar, K. J. *Cellulose* **2007**, *14*, 49–64.
(20) Badulescu, R.; Vivod, V.; Jausovec, D.; Voncina, B *Carbohyd. Polym.* **2008**, *71*, 85–91.
(21) Salaün, F.; Devaux, E.; Bourbigot, S.; Rumeau, P. *Carbohyd. Polym.* **2010**, *79*, 964–974.
(22) Bras, M. L.; Bourbigot, S.; Félix, E.; Pouille, F.; Traisnel, C. *Polymer* **2000**, *41*, 5283–5296.
(23) Bourbigot, S.; Bras, M. L.; Dabrowski, F.; Gilman, J. W.; Kashiwagi, T. *Fire Mater.* **2000**, *24*, 201–208.
(24) Weil, E. D.; Hirschler, M. M.; Patel, N. G.; Said, M. M.; Shakir, S. *Fire Mater.* **1992**, *16*, 159–167.